Journal of Animal and Feed Sciences, https://doi.org/10.22358/jafs/225576/2026
The Kielanowski Institute of Animal Physiology and Nutrition, Polish Academy of Sciences, Jabłonna

ORIGINAL PAPER

ARTICLE IN PRESS

(final version of manuscript before type-setted PDF)

Small-intestinal microbiota patterns in growing Hu sheep fed low-protein diets with rumen-protected lysine and methionine

R. Jan[1,*], Z. Yu[1], M. Iftikhar[1], M. Hammad Zafar[1], X. Zhong[1], X. Zhang[2] and M. Wang[1]

[1] Yangzhou University, College of Animal Sciences and Technology, Yangzhou 225009, China

[2] State Key Laboratory of Sheep Genetic Improvement and Healthy Production, Xinjiang Academy of Agricultural Reclamation Sciences, Shihezi, Xinjiang 832000, China

*Corresponding authors:
e-mail: zhangx0322@126.com, mengzhiwangyz@126.com

Short title: Segment-specific gut microbiota in sheep

Received: 26 May 2026
Revised: 6 July 2026
Accepted: 7 July 2026

ABSTRACT. Dietary crude protein reduction and supplementation with rumen-protected amino acids may improve nitrogen utilisation in sheep; however, their effects on different small-intestinal sites remain unknown. This study investigated the digesta microbiota in paired duodenal and jejunal samples from 38 growing male Hu sheep fed one of four experimental diets: a conventional protein control diet, a low-protein diet (LPD), an LPD supplemented with rumen-protected lysine (LPDL), and an LPD supplemented with rumen-protected methionine (LPDM). Overall, 76 paired

digesta samples representing 38 matched duodenum-jejunum pairs were analysed using 16S rRNA gene sequencing, and PICRUSt2 was employed to predict microbial functional potential. Host-response parameters, including serum biochemical, antioxidant, and immune-related indicators, were analysed to provide additional physiological context. In both intestinal segments, dietary treatment had no effect on alpha diversity. Richness-based indices, community structure (Bray-Curtis), dominant taxa, and inferred functional potential differed between the duodenal and jejunal communities. The effect of intestinal segment was greater than that of dietary treatment, and taxonomic and predicted functional differences associated with diet were observed primarily in the jejunum. Serum catalase activity differed between treatments after false discovery rate correction, with lower activity in the LPDM group; however, this finding was considered contextual rather than mechanistic. Overall, intestinal segments showed a stronger association with the small-intestinal microbial pattern than dietary treatment, suggesting that the duodenal and jejunal microbiota should be investigated separately in ruminant nutritional trials.

KEY WORDS: 16S rRNA sequencing, amino acid supplementation, bacterial community, functional inference, Hu sheep, nitrogen utilization

Introduction

The gastrointestinal microbiome plays a major role in ruminant nutrition, health (Rawal et al., 2024) and productivity by contributing to feed conversion, microbial metabolite production, nitrogen cycling and host physiological regulation (Wang et al., 2019; Abdallah et al., 2020; Cholewińska et al., 2021). Although research has focused primarily on the rumen and faeces, the small intestine is essential for digestion, absorption, maintenance of epithelial integrity and host–microbial interaction (Pereira and Berry, 2017; Cholewińska et al., 2020). Low-protein diets supplemented with limiting amino acids may improve nitrogen utilization; however, their

segment-specific effects on the small-intestinal microbiota remain poorly understood (Gebeyew et al., 2021; Zhang et al., 2022; Wei et al., 2023).

The small intestine is not a homogeneous environment, and dietary interventions can affect microbial composition differently in individual regions (Wang et al., 2025; Zhang et al., 2025). The duodenum receives acidic digesta, bile, pancreatic secretions and variable substrates, while the jejunum is the main site of enzymatic digestion and nutrient absorption and is characterised by a distinct luminal environment (Basile et al., 2025). These regional differences in luminal conditions, microbial communities and epithelial physiology, which are sensitive to nutritional stress in sheep (Wu et al., 2025), justify separate evaluation of the duodenum and jejunum intestinal segments.

The objective of the present study was to describe intestinal microbiota in the duodenum and jejunum under different dietary treatments and to determine whether low-protein diets with rumen-protected lysine or methionine are associated with uniform or segment-specific microbial responses. Serum biochemical, antioxidant and immune-related markers were also assessed to provide additional host-response context.

Material and methods

Ethics statement and animal source

All animal procedures were approved by the Animal Care and Use Committee of Yangzhou University approved on 7 April 2023 (Approval Code: 202302007). The experiment was conducted at the Sheep Research Center of Yangzhou University in Yangzhou, Jiangsu, China from September 2024 to January 2025. No antibiotics were administered during the experimental

period. The sheep were purchased specifically for this study and were housed and managed by Yangzhou University throughout the experiment. Therefore, informed consent from a private owner was not applicable.

Animal management and experimental design

Thirty-eight 3-month-old male Hu sheep (23.6 ± 2.10 kg) were used in the trial. The sheep were housed individually in pens equipped with feed tubs and nipple drinkers, and water was provided *ad libitum* (Figure 1). Feed was offered twice daily at 08:30 and 16:30 h, and refusals were collected once a day before the morning feeding. The experiment was conducted in a randomized block design and lasted 10 weeks, comprising a 2-week covariate period followed by an 8-week experimental period. The overall study design and analytical workflow are shown in Figure 2. The same animals were used throughout the feeding trial, and measurements of body weight, feed intake, feed conversion ratio, apparent digestibility and rumen fermentation were included as nutritional context for the interpretation of the microbiome data

Diets and treatments

During the covariate period, all sheep were fed a commercial pelleted total mixed ration. Subsequently, the animals were randomly allocated to one of four dietary treatments: (1) a conventional-protein diet (CTRL, 14.0% crude protein [CP]); (2) a low-protein diet (LPD, 11.4% CP); (3) an LPD supplemented with rumen-protected lysine (LPDL, 15 g/day); and (4) an LPD supplemented with rumen-protected methionine (LPDM, 0.59% of dietary dry matter [DM]). All diets were provided as pelleted total mixed rations. The rumen-protected lysine and methionine products were AjiPro-L and MetaSmart, respectively.

Serum sampling and intestinal digesta collection

Serum biochemical, antioxidant, and immune-related parameters were quantified using commercially available assay kits. Glucose was measured using the glucose oxidase–peroxidase (GOPOD) enzymatic method (520 nm). Antioxidant enzymes included catalase (CAT; ADS-W-KY002), superoxide dismutase (SOD; WST-8 method, ADS-W-KY011), glutathione peroxidase (GSH-Px; ADS-W-G003) and reduced glutathione (GSH; ADS-W-G001), using kits supplied by Jiangsu Addison Biotechnology Co., Ltd., Nanjing, Jiangsu Province, China. Immune-related markers, including immunoglobulin A (IgA), immunoglobulin M (IgM), interleukin-1β (IL-1β), interleukin-2 (IL-2), interleukin-4 (IL-4), interleukin-10 (IL-10), tumour necrosis factor-α (TNF-α) and interferon-γ (IFN-γ), were measured using sheep-specific sandwich enzyme-linked immunosorbent assay (ELISA) kits purchased from Jiangsu Meimian Industrial Co., Ltd. (Yancheng, China). All assays were performed according to the manufacturers' instructions. Details of the assay principles, wavelengths or detection ranges, catalogue information, and intra- and inter-assay coefficients of variation (CVs) are provided in Supplementary Table S1. The ELISA kits were sheep-specific.

Absorbance was measured at 450 nm using a microplate reader, and concentrations were calculated from standard curves. These serum variables were considered supportive indicators of the host response rather than primary mechanistic endpoints.

Sheep were fasted for 24 h prior to slaughter, with free access to water to standardise gut fill and reduce variation in digesta volume between animals. This fasting period was intended to improve the comparability of intestinal digesta sampling across treatments; however, it may have influenced microbial composition and was therefore taken into account when interpreting the results. Animals were slaughtered by exsanguination according to the approved institutional animal-use protocol. Immediately after slaughter and opening of the abdominal cavity, duodenal

and jejunal digesta samples were collected from each animal, resulting in true paired within-animal sampling. Each sheep was a donor of one duodenal and one jejunal sample. The duodenum was identified with reference to the pylorus of the abomasum and the duodenal flexure, whereas the jejunum was sampled from a standardised mid-small-intestinal site distal to the duodenojejunal flexure. To minimise cross-contamination, intestinal segments were sampled separately using sterile instruments, which were replaced or disinfected between sampling sites. Digesta aliquots were gently homogenised, transferred to sterile cryovials, immediately frozen in liquid nitrogen, transported to the laboratory, and stored at −80 °C until DNA extraction.

DNA extraction, sequencing, and bioinformatics

Microbial genomic DNA was extracted from digesta samples using the MagPure Soil DNA LQ Kit (Magen, Guangzhou, China). DNA concentration and purity were assessed using a NanoDrop 2000 spectrophotometer, and DNA integrity was evaluated by agarose gel electrophoresis. The V3–V4 hypervariable region of the bacterial 16S rRNA gene was amplified using the primers 343F (5′-TACGGRAGGCAGCAG-3′) and 798R (5′-AGGGTATCTAATCCT-3′).

Amplicons were verified by agarose gel electrophoresis, purified using Agencourt AMPure XP paramagnetic beads (Beckman Coulter, Brea, CA, USA), quantified using a Qubit double-stranded DNA (dsDNA) assay kit, pooled, and sequenced on an Illumina NovaSeq 6000 platform (paired-end, 2 × 250 bp) by OE Biotech Co., Ltd. (Shanghai, China). Raw FASTQ files were processed using the DADA2 (Divisive Amplicon Denoising Algorithm 2) pipeline implemented in QIIME 2 (Quantitative Insights Into Microbial Ecology 2), version 2020.11 (Bolyen et al., 2019). Primer sequences were removed using Cutadapt (Martin, 2011), and chimeric sequences were identified and removed within the DADA2 pipeline.

Amplicon sequence variants (ASVs) were inferred, and an ASV abundance table was generated. Taxonomic assignment was performed using the q2-feature-classifier plugin (Bokulich et al., 2018) with the SILVA 138 ribosomal RNA (rRNA) gene database (Quast et al., 2013). PICRUSt2 was used to infer the functional potential of the microbial communities based on 16S rRNA gene profiles. These predictions represent estimates of gene family abundance rather than direct measurements of microbial activity, gene expression, or metabolite production.

Therefore, all functional outputs should be interpreted as inferred functional potential rather than experimentally validated metabolic activity. Confirmation of these predictions would require complementary metagenomic, metatranscriptomic or metabolomic analyses.

Statistical analysis

Samples were classified according to intestinal segment (duodenum or jejunum), dietary treatment (CTRL, LPD, LPDL, or LPDM), and paired animal ID. Alpha-diversity indices are presented as mean ± standard deviation (SD). Within each intestinal segment, the effects of dietary treatment were analysed using Kruskal-Wallis tests, followed by false discovery rate (FDR) correction (Benjamini and Hochberg, 1995) across the multiple alpha-diversity metrics.

Because samples were paired within individual animals, Wilcoxon signed-rank tests were used to compare duodenal and jejunal samples. All statistical results are reported as raw *P*-values followed by Benjamini-Hochberg FDR-adjusted q-values. Statistical significance was defined as $q < 0.05$, while $0.05 \leq q < 0.10$ was considered a statistical trend.

Principal coordinate analysis (PCoA) and permutational multivariate analysis of variance (PERMANOVA) (Anderson, 2001), based on Bray-Curtis distances, were used to assess community structure. The PERMANOVA model included intestinal segment, dietary treatment, and their interaction (segment × treatment), and effect sizes are reported as R^2 values. FDR

correction was applied to taxonomic features and Phylogenetic Investigation of Communities by Reconstruction of Unobserved States version 2 (PICRUSt2)-inferred Kyoto Encyclopedia of Genes and Genomes (KEGG) profiles.

PICRUSt2 functional predictions were interpreted cautiously as inferred functional potential and were not validated using metagenomic, metatranscriptomic, or metabolomic data. Serum markers were compared using Kruskal-Wallis tests, and post-hoc pairwise Mann-Whitney tests were adjusted for FDR where applicable.

Results

Sample structure and sequencing depth

The final microbiome dataset consisted of paired duodenal and jejunal digesta samples from 38 sheep. The number of animals per treatment group was as follows: CTRL (n = 9), LPD (n = 11), LPDL (n = 8), and LPDM (n = 10). Each sheep provided one duodenal and one jejunal digesta sample, resulting in 38 paired sample sets and 76 microbiome samples. The same treatment-group distribution was represented in each intestinal segment (Table 1), allowing paired comparisons between the two small-intestinal segments.

A total of 12008 amplicon sequence variants (ASVs) were detected in the non-rarefied dataset, of which 11110 were retained after processing. The number of observed ASVs ranged from 129.0 to 948.8 across the 76 samples. Shannon diversity ranged from 3.16 to 8.17, and sequencing coverage was high (mean Good's coverage ≈ 0.999). Rarefaction curves approached a plateau (Supplementary Figure S1), indicating that sequencing depth was sufficient for downstream diversity analyses.

Alpha diversity varied mainly by intestinal segment

Alpha diversity did not differ significantly between dietary treatments in either the duodenum or jejunum (Table 2). These results indicate that no detectable effect of diet on alpha diversity was observed under the conditions of this study.

In contrast, paired comparisons between intestinal segments showed significant differences in richness-based indices. ASVs, Chao1 richness, and Faith's phylogenetic diversity remained significant after FDR correction, whereas the Shannon and Simpson diversity indices and Good's coverage did not differ significantly between the duodenum and jejunum. These results imply that intestinal segment contributed more to variation in alpha-diversity than dietary treatment (Figure 3).

Overall, intestinal segment explained a larger proportion of the variation in microbial community structure than dietary treatment, although both factors contributed significantly (Figure 4).

Beta diversity supported segment-specific community structure

PERMANOVA indicated that intestinal segment was the primary factor explaining variation in microbial community structure ($R^2 = 0.109$, $P = 0.001$), whereas dietary treatment explained a smaller but statistically significant proportion of the variation ($R^2 = 0.068$, $P = 0.001$). A significant segment × treatment interaction was also detected ($R^2 = 0.085$, $P = 0.001$), indicating that the effect of dietary treatment on the microbial community differed between intestinal segments (Table 3).

Segment-specific differences in taxonomic composition

The predominant bacterial phyla were Bacteroidota, Firmicutes, Proteobacteria, Actinobacteriota, and Fusobacteriota. Firmicutes had a higher mean relative abundance in the jejunum, whereas Proteobacteria was more abundant in the duodenum. At the genus level, *Ruminobacter* and *Prevotella* were abundant in the duodenum, while *Alistipes* was more abundant in the jejunum. The phylum- and genus-level taxa showing the strongest differences between the paired intestinal segments after FDR correction are presented in Table 4. The relative abundance of the dominant phyla in dietary treatments are shown in Figure 5 and Supplementary Table S5.

Segment- and diet-associated taxa

Numerous taxa were significantly associated with intestinal segment after FDR correction, indicating marked differences in microbial composition between the duodenum and jejunum. In contrast, diet-associated differences at the genus level were observed primarily in the jejunum. The taxa associated with intestinal segment and dietary treatment are presented in Figure 6.

PICRUSt2-predicted functional profiles

The 16S rRNA gene profiles were used to infer microbial functional potential using PICRUSt2. The dominant KEGG Level 2 categories included global and overview maps, carbohydrate metabolism, amino acid metabolism, metabolism of cofactors and vitamins, energy metabolism, translation, membrane transport, replication and repair, nucleotide metabolism, and glycan biosynthesis and metabolism. After FDR correction, significant differences between the duodenum and jejunum were observed for global and overview maps, amino acid metabolism, metabolism of cofactors and vitamins, and energy metabolism (Table 5). Diet-associated differences in inferred functional potential were mainly observed in the jejunum and involved categories related to cell motility and protein processing, such as protein folding, sorting, and degradation. Because these results represent predicted functional potential rather than directly

measured microbial activity, they should be interpreted cautiously and validated in future studies using metagenomics, transcriptomics, or metabolomics.

Serum host-response indicators

Thirty-eight serum samples were analysed to assess biochemical, antioxidant, and immune-related responses in the four dietary treatments. Catalase activity differed significantly between treatments after FDR correction, with the lowest value observed in the LPDM group. No other serum marker remained significant after FDR adjustment (Table 6; Figure 7). These serum variables were treated as supportive host-response indicators rather than primary mechanistic endpoints.

Nutritional characteristics of the sequenced animals

Growth performance, feed intake, feed conversion, nutrient digestibility, and rumen fermentation data of the 38 sequenced sheep are provided in Supplementary Tables S2–S4. These measurements were used to provide background information for interpretation of microbiome results and to ensure microbial patterns were considered in conjunction with animal-level nutritional responses. These performance, digestibility, and fermentation data are included as ancillary data and are not considered primary endpoints, as the main objective of this study was the comparison of duodenal and jejunal microbiota.

Discussion

This study showed that small-intestinal microbiota composition and PICRUSt2-inferred functional potential differed mainly between intestinal segments in growing Hu sheep. The paired duodenal–jejunal sampling method enabled direct comparison of two compartments of the small

intestine within the same animals. Overall, differences between intestinal segments were more pronounced and consistent than those associated with dietary treatment, and diet-related changes were detected more frequently in the jejunum than in the duodenum.

No significant effect of dietary treatment on alpha diversity was detected after FDR correction in either intestinal segment. However, this should be interpreted as a lack of detectable diet-related differences rather than evidence of equivalence or the complete absence of dietary effects. The moderate sample size may have limited the ability to detect smaller treatment effects. In contrast, paired comparisons between intestinal segments revealed significant differences in richness-based indices, suggesting that intestinal segment is a stronger determinant of alpha diversity than dietary intervention.

Marked taxonomic differences were also observed between intestinal segments. Firmicutes had a higher relative abundance in the jejunum, whereas Proteobacteria were more numerous in the duodenum. These findings are consistent with the distinct physiological conditions of the two intestinal segments, including differences in exposure to gastric outflow, bile and pancreatic secretions, digesta flow, substrate availability, epithelial absorption, and immune signalling. Multiple taxa also differed significantly between the duodenum and jejunum after FDR correction.

Diet-related taxonomic and inferred functional differences were observed primarily in the jejunum. This suggests that the mid-small-intestinal environment may be more responsive to protein reduction and rumen-protected amino acid supplementation than the duodenum. However, these findings should be interpreted with caution, as they were detected against a stronger segment effect, involved multiple low- to moderate-abundance taxa, and functional categories, and were not accompanied by significant diet-related differences in alpha diversity after FDR correction.

Serum markers were included to provide additional host-response context. Catalase activity differed between dietary treatments, with the lowest activity observed in the LPDM group, while other serum markers were not significant after FDR correction. Catalase plays an important role in antioxidant defence and redox homeostasis; therefore, the reduced CAT activity in LPDM may reflect changes in host oxidative status. However, this finding should not be regarded as direct mechanistic evidence of microbiota-driven functional changes, as no significant differences were observed in the other antioxidant or immune-related markers, and the serum variables represented secondary outcomes.

Duodenal and jejunal digesta samples were collected from the same animals at slaughter, resulting in true within-animal paired sampling. Each sheep was a donor of one duodenal and one jejunal sample, allowing direct paired comparison of the two intestinal segments under identical host and dietary conditions. This paired design enabled segment-specific comparisons while minimising between-animal variation. Although PERMANOVA showed a significant segment × treatment interaction, the effect size of dietary treatment was smaller than that of intestinal segment, indicating that intestinal segment was the primary determinant of microbial variation.

This study has several limitations that should be considered when interpreting the results. First, the sample size per treatment group (n = 8–11) may have limited the statistical power to detect subtle dietary effects. Second, the 24-hour fasting period prior to slaughter may have influenced digesta flow and microbial activity in the small intestine. Third, PICRUSt2-based functional predictions represent inferred gene content rather than directly measured microbial activity. Fourth, serum biochemical and antioxidant markers were included as supportive host-response indicators rather than mechanistic endpoints. Finally, metagenomic, metabolomic, and intestinal nutrient flux analyses were not performed, limiting mechanistic interpretation.

Conclusions

This analysis of paired duodenal and jejunal samples showed that intestinal segment was a stronger determinant of the small-intestinal microbiota than dietary treatment in growing Hu sheep. Differences between the duodenum and jejunum were consistently observed in microbial richness, community structure, taxonomic composition, and predicted functional potential. In contrast, diet-related taxonomic and predicted functional differences were detected only in the jejunum, whereas no significant dietary effects on alpha diversity were observed in either intestinal segment. These findings highlight the importance of analysing the duodenum and jejunum separately when evaluating dietary interventions in ruminants. Further studies using metagenomics, transcriptomics, metabolomics, and mucosal sampling are needed to validate the predicted functional profiles and clarify the underlying mechanisms.

Conflict of interest

The Authors declare that there is no conflict of interest.

Funding

This work was supported by the Bintuan Key R&D Project (2024AB033, 2023AB078), the Ministry of Science and Technology of China's High-end Foreign Experts Program (H20250797), the Huaian Talent Enclave Expert Workstation Program, and the Priority Academic Program Development of Jiangsu Higher Education Institution (PAPD), P.R. China. Laboratory facilities and equipment were provided by the College of Animal Science and Technology, Yangzhou University, China.

Acknowledgements

The authors would like to thank the College of Animal Science and Technology, Yangzhou University, China, for support and laboratory facilities.

References

Abdallah A., Elemba E., Zhong Q., Sun Z., 2020. Gastrointestinal interaction between dietary amino acids and gut microbiota: with special emphasis on host nutrition. Curr. Protein Pept. Sci. 21, 785–798, https://doi.org/10.2174/1389203721666200212095503

Anderson M.J., 2001. A new method for non-parametric multivariate analysis of variance. Austral Ecol. 26, 32–46, https://doi.org/10.1111/j.1442-9993.2001.01070.pp.x

Basile E.J., Shukla K., Launico M.V., Sheer A.J., 2025. Physiology, nutrient absorption. In: StatPearls [Internet]. StatPearls Publishing. Treasure Island, FL (USA). Available from: https://www.ncbi.nlm.nih.gov/books/NBK597379/

Benjamini Y., Hochberg Y., 1995. Controlling the false discovery rate: a practical and powerful approach to multiple testing. J. R. Stat. Soc. Ser. B Methodol. 57, 289–300, https://doi.org/10.1111/j.2517-6161.1995.tb02031.x

Bokulich N.A., Kaehler B.D., Rideout J.R., Dillon M., Bolyen E., Knight R., Huttley G.A., Caporaso J.G., 2018. Optimizing taxonomic classification of marker-gene amplicon sequences with QIIME 2's q2-feature-classifier plugin. Microbiome 6, 90, https://doi.org/10.1186/s40168-018-0470-z

Bolyen E., Rideout J.R., Dillon M.R. et al., 2019. Reproducible, interactive, scalable and extensible microbiome data science using QIIME 2. Nat. Biotechnol. 37, 852–857, https://doi.org/10.1038/s41587-019-0209-9

Cholewińska P., Czyż K., Nowakowski P., Wyrostek A., 2020. The microbiome of the digestive system of ruminants: a review. Anim. Health Res. Rev. 21, 3–14, https://doi.org/10.1017/S1466252319000069

Cholewińska P., Górniak W., Wojnarowski K., 2021. Impact of selected environmental factors on microbiome of the digestive tract of ruminants. BMC Vet. Res. 17, 25, https://doi.org/10.1186/s12917-021-02742-y

Gebeyew K., Yang C., He Z., Tan Z., 2021. Low-protein diets supplemented with methionine and lysine alter the gut microbiota composition and improve the immune status of growing lambs. Appl. Microbiol. Biotechnol. 105, 8393–8410, https://doi.org/10.1007/s00253-021-11620-4

Martin M., 2011. Cutadapt removes adapter sequences from high-throughput sequencing reads. EMBnet.journal 17, 10–12, https://doi.org/10.14806/ej.17.1.200

Pereira F.C., Berry D., 2017. Microbial nutrient niches in the gut. Environ. Microbiol. 19, 1366–1378, https://doi.org/10.1111/1462-2920.13659

Quast C., Pruesse E., Yilmaz P., Gerken J., Schweer T., Yarza P., Peplies J., Glöckner F.O., 2013. The SILVA ribosomal RNA gene database project: improved data processing and web-based tools. Nucleic Acids Res. 41, D590–D596, https://doi.org/10.1093/nar/gks1219

Rawal S., Kaur H., Bhathan S., Mittal D., Kaur G., Ali S.A., 2024. Ruminant gut microbiota: interplay, implications, and innovations for sustainable livestock production. In: V.K. Yata, A.K. Mohanty, E. Lichtfouse (Editors). Sustainable Agriculture Reviews: Animal Biotechnology for Livestock Production 4. Springer Nature. Cham (Switzerland), pp. 205–228, https://doi.org/10.1007/978-3-031-54372-2_7

Wang L., Liu K., Wang Z., Bai X., Peng Q., Jin L., 2019. Bacterial community diversity associated with different utilization efficiencies of nitrogen in the gastrointestinal tract of goats. Front. Microbiol. 10, 239, https://doi.org/10.3389/fmicb.2019.00239

Wang X.L., Zhou J., Lu M.L., Zhao S.P., Li W.J., Quan G.B., Xue B., 2025. Mucosal barrier function and microbial community of small intestines in sheep in response to dietary energy concentrations. Animal 19, 101550, https://doi.org/10.1016/j.animal.2025.101550

Wei X., Wu H., Wang Z., Zhu J., Wang W., Wang J., Wang Y., Wang C., 2023. Rumen-protected lysine supplementation improved amino acid balance, nitrogen utilization and altered hindgut microbiota of dairy cows. Anim. Nutr. 15, 320–331, https://doi.org/10.1016/j.aninu.2023.08.001

Wu W., Akhtar M.F., Geng J., Lu H., Rahim M.A., Cheng J., Ding X., Mao S., Xue Y., 2025. Undernutrition disrupts jejunal and ileal microbiota and epithelial tissue homeostasis in a pregnant sheep model. Anim. Nutr. 20, 263–276, https://doi.org/10.1016/j.aninu.2024.10.004

Zhang F., Wu Z., Zhang Y., Su Q., Zhu K., Chen X., Hou S., Gui L., 2025. Different lysine-to-methionine ratios in a low-protein diet affect the microbiome and metabolome, influencing the jejunal barrier function in Tibetan sheep. Front. Microbiol. 16, 1441143, https://doi.org/10.3389/fmicb.2025.1441143

Zhang Z., Shahzad K., Shen S. et al., 2022. Altering dietary soluble protein levels with decreasing crude protein may be a potential strategy to improve nitrogen efficiency in Hu sheep based on rumen microbiome and metabolomics. Front. Nutr. 8, 815358, https://doi.org/10.3389/fnut.2021.815358

Table 1. Sample structure

Segment	CTRL	LPD	LPDL	LPDM	Total
Duodenum	9	11	8	10	38
Jejunum	9	11	8	10	38
Total	18	22	16	20	76

CTRL – conventional-protein control diet, LPD – low-protein diet, LPDL – low-protein diet supplemented with rumen-protected lysine, LPDM – low-protein diet supplemented with rumen-protected methionine. Each animal contributed one duodenal and one jejunal digesta sample. Therefore, the same dietary group sizes are shown for both intestinal segments, representing true paired samples from the same animals.

Table 2. Alpha-diversity indices in duodenal and jejunal digesta samples by dietary treatment

Metric	Segment	CTRL	LPD	LPDL	LPDM	Diet *P* / q	Segment *P* / q
Shannon	Duodenum	7.00 ± 0.94[a]	6.12 ± 0.93[a]	5.83 ± 1.42[a]	6.51 ± 0.91[a]	0.094 / 0.282	0.989 / 0.989
Shannon	Jejunum	5.99 ± 0.92[a]	6.70 ± 0.75[a]	6.46 ± 0.24[a]	6.42 ± 0.42[a]	0.099 / 0.198	
Observed ASVs	Duodenum	468.57 ± 153.06[a]	443.66 ± 166.44[a]	412.81 ± 163.51a	453.56 ± 169.62[a]	0.943 / 0.957	0.010 / 0.025
Observed ASVs	Jejunum	420.93 ± 224.22[a]	333.47 ± 95.16[a]	326.35 ± 54.64[a]	302.27 ± 90.76[a]	0.646 / 0.646	
Simpson	Duodenum	0.960 ± 0.063[a]	0.941 ± 0.034[a]	0.897 ± 0.105[a]	0.958 ± 0.034[a]	0.071 / 0.282	0.204 / 0.245
Simpson	Jejunum	0.934 ± 0.040[a]	0.967 ± 0.037[a]	0.973 ± 0.007[a]	0.971 ± 0.019[a]	0.031 / 0.125	
Chao1	Duodenum	479.46 ± 161.49[a]	456.53 ± 173.16[a]	426.59 ± 166.86[a]	466.50 ± 174.90[a]	0.957 / 0.957	0.012 / 0.025
Chao1	Jejunum	440.11 ± 237.90[a]	340.40 ± 99.11[a]	332.71 ± 56.27[a]	307.77 ± 94.35[a]	0.577 / 0.646	
Faith's PD	Duodenum	44.46 ± 9.92[a]	43.15 ± 10.71[a]	39.30 ± 12.32[a]	44.06 ± 13.49[a]	0.763 / 0.957	2.00e-04 / 0.001
Faith's PD	Jejunum	38.07 ± 17.05[a]	31.00 ± 7.61[a]	31.43 ± 4.55[a]	28.54 ± 6.15[a]	0.587 / 0.646	
Good's coverage	Duodenum	0.999 ± 0.001[a]	0.999 ± 0.001[a]	0.999 ± 0.001[a]	0.999 ± 0.000[a]	0.914 / 0.957	0.067 / 0.101
Good's coverage	Jejunum	0.998 ± 0.001[a]	0.999 ± 0.000[a]	0.999 ± 0.000[a]	0.999 ± 0.000[a]	0.042 / 0.125	

CTRL – conventional-protein control diet, LPD – low-protein diet, LPDL – low-protein diet supplemented with rumen-protected lysine, LPDM – low-protein diet supplemented with rumen-protected methionine, ASVs – amplicon sequence variants, PD – phylogenetic diversity, FDR – false discovery rate. Values are presented as mean ± standard deviation. Group sizes within each intestinal segment were CTRL, n = 9; LPD, n = 11; LPDL, n = 8; and LPDM, n = 10. Diet *P*-values were obtained using Kruskal-Wallis tests within each segment, and diet q-values are Benjamini-Hochberg false discovery rate (FDR)-adjusted values. Segment *P*-values were obtained using paired Wilcoxon signed-rank tests comparing the duodenum and jejunum, and segment q-values are FDR-adjusted values. Identical superscript letters indicate no significant post-hoc difference among dietary treatments within the same intestinal segment. Statistical significance was defined as $q < 0.05$.

Table 3. PERMANOVA of Bray-Curtis community structure using intestinal segment, dietary treatment, and their interaction

Factor	pseudo-F	R^2	*P*	Interpretation
Segment	10.0565	0.1092	0.001	Segment effect; stronger than diet.
Treatment	2.0703	0.0675	0.001	Small treatment effect.
Segment × treatment	2.6005	0.0847	0.001	Formal interaction term; responses differed by segment.

PERMANOVA – permutational multivariate analysis of variance, pseudo-F – pseudo-F statistic, R^2 – proportion of variance explained, *P* – permutation probability value. PERMANOVA was performed using the even feature table and Bray-Curtis dissimilarity distances. The model included intestinal segment, dietary treatment, and the segment × treatment interaction. Effect sizes are reported as R^2 values, representing the proportion of microbial community variation explained by each factor. The *P*-values are permutation-based values calculated using 999 permutations

Table 4. Strongest segment-associated phylum- and genus-level signals in paired duodenal and jejunal samples

Rank	Taxon	Duodenum mean, %	Jejunum mean, %	*P*	q
Phylum	Firmicutes	23.142431	38.663834	1.39e-07	2.57e-06
Phylum	Proteobacteria	24.312716	8.340212	9.44e-08	2.57e-06
Phylum	Fibrobacterota	0.533812	0.009786	5.91e-07	7.29e-06
Phylum	Spirochaetota	0.701474	0.0753	4.05e-06	3.75e-05
Phylum	Elusimicrobiota	0.039788	0.001996	9.84e-06	7.28e-05
Phylum	Deferribacterota	0.054728	0.426175	7.03e-05	4.34e-04
Phylum	Desulfobacterota	0.584593	0.708578	0.004	0.019
Genus	*Ruminobacter*	8.981345	0.023676	7.28e-12	5.48e-09
Genus	*Prevotella*	10.891983	1.097379	4.66e-09	1.75e-06
Genus	*Alistipes*	0.348333	4.416168	7.24e-08	1.36e-05
Genus	*Rikenellaceae_RC9_gut_group*	2.087551	0.422861	6.33e-08	1.36e-05
Genus	*NK4A214_group*	0.680653	0.042476	2.02e-07	3.05e-05

FDR – false discovery rate. Values represent the mean relative abundance (%) of each taxon in paired duodenal and jejunal digesta samples. The *P*-values were obtained from paired comparisons between the duodenum and jejunum, and the q-values are Benjamini-Hochberg false discovery rate-adjusted values calculated within each taxonomic rank. The direction of each difference should be interpreted by comparing the mean relative abundances in the two intestinal segments.

Table 5. Dominant PICRUSt2-inferred KEGG Level 2 categories across duodenal and jejunal samples

KEGG Level 2 category	Overall mean, %	Duodenum (CTRL; LPD; LPDL; LPDM)	Jejunum (CTRL; LPD; LPDL; LPDM)	Segment *P* / q
Global and overview maps	43.583372	CTRL: 43.70 ± 0.40; LPD: 43.79 ± 0.34; LPDL: 43.76 ± 0.43; LPDM: 43.78 ± 0.33	CTRL: 43.70 ± 0.28; LPD: 43.39 ± 0.34; LPDL: 43.42 ± 0.17; LPDM: 43.16 ± 0.72	5.34e-04 / 0.004
Carbohydrate metabolism	9.213661	CTRL: 8.83 ± 0.35; LPD: 9.28 ± 0.51; LPDL: 9.12 ± 0.45; LPDM: 9.33 ± 0.71	CTRL: 9.63 ± 0.88; LPD: 9.15 ± 0.30; LPDL: 9.16 ± 0.07; LPDM: 9.20 ± 0.39	0.464 / 0.540
Amino acid metabolism	6.31742	CTRL: 6.19 ± 0.08; LPD: 6.24 ± 0.12; LPDL: 6.30 ± 0.24; LPDM: 6.24 ± 0.12	CTRL: 6.30 ± 0.15; LPD: 6.43 ± 0.11; LPDL: 6.45 ± 0.05; LPDM: 6.41 ± 0.30	2.64e-05 / 3.17e-04
Metabolism of cofactors and vitamins	4.132829	CTRL: 4.34 ± 0.20; LPD: 4.25 ± 0.21; LPDL: 4.16 ± 0.31; LPDM: 4.16 ± 0.14	CTRL: 3.98 ± 0.31; LPD: 4.05 ± 0.15; LPDL: 4.10 ± 0.11; LPDM: 4.02 ± 0.24	7.26e-04 / 0.004
Energy metabolism	3.815749	CTRL: 3.89 ± 0.11; LPD: 3.87 ± 0.08; LPDL: 3.78 ± 0.24; LPDM: 3.87 ± 0.11	CTRL: 3.77 ± 0.17; LPD: 3.76 ± 0.10; LPDL: 3.78 ± 0.05; LPDM: 3.79 ± 0.06	0.004 / 0.015
Translation	3.102936	CTRL: 3.25 ± 0.12; LPD: 2.99 ± 0.27; LPDL: 3.19 ± 0.11; LPDM: 3.02 ± 0.42	CTRL: 3.01 ± 0.52; LPD: 3.14 ± 0.22; LPDL: 3.11 ± 0.13; LPDM: 3.15 ± 0.19	0.989 / 0.989
Membrane transport	2.956507	CTRL: 2.85 ± 0.33; LPD: 2.79 ± 0.20; LPDL: 2.99 ± 0.48; LPDM: 3.04 ± 0.36	CTRL: 3.25 ± 0.65; LPD: 3.03 ± 0.28; LPDL: 2.77 ± 0.16; LPDM: 2.93 ± 0.42	0.287 / 0.382
Replication and repair	2.827104	CTRL: 2.91 ± 0.13; LPD: 2.76 ± 0.17; LPDL: 2.88 ± 0.07; LPDM: 2.78 ± 0.27	CTRL: 2.79 ± 0.36; LPD: 2.85 ± 0.16; LPDL: 2.81 ± 0.10; LPDM: 2.85 ± 0.18	0.852 / 0.930
Nucleotide metabolism	2.619875	CTRL: 2.66 ± 0.05; LPD: 2.59 ± 0.08; LPDL: 2.68 ± 0.06; LPDM: 2.61 ± 0.15	CTRL: 2.69 ± 0.25; LPD: 2.61 ± 0.12; LPDL: 2.56 ± 0.04; LPDM: 2.57 ± 0.09	0.215 / 0.295
Glycan biosynthesis and metabolism	2.479454	CTRL: 2.49 ± 0.08; LPD: 2.73 ± 0.26; LPDL: 2.41 ± 0.33; LPDM: 2.45 ± 0.29	CTRL: 2.45 ± 0.32; LPD: 2.39 ± 0.17; LPDL: 2.48 ± 0.12; LPDM: 2.39 ± 0.16	0.067 / 0.120

KEGG – Kyoto Encyclopedia of Genes and Genomes, CTRL – conventional-protein control diet, LPD – low-protein diet, LPDL – low-protein diet supplemented with rumen-protected lysine, LPDM – low-protein diet supplemented with rumen-protected methionine, FDR – false discovery rate, SD – standard deviation, PICRUSt2 – Phylogenetic Investigation of Communities by Reconstruction of Unobserved States 2. Values are presented as mean ± SD. The overall mean represents the average relative abundance of each PICRUSt2-inferred KEGG Level 2 category across

all 76 samples. Segment p-values were obtained from paired duodenum-jejunum comparisons, and segment q-values are Benjamini-Hochberg false discovery rate (FDR)-adjusted values. Statistical significance was defined as $q < 0.05$

Table 6. Serum biochemical, antioxidant, and immune-related indices across dietary groups (mean ± SD)

Marker	CTRL	LPD	LPDL	LPDM	*P*	q
Glucose, mg/ml	0.84 ± 0.10[a]	0.85 ± 0.11[a]	0.91 ± 0.09[a]	0.90 ± 0.16[a]	0.340	0.655
CAT, μmol/min/ml	4.00 ± 0.48[a]	4.40 ± 0.91[a]	4.61 ± 0.66[a]	3.31 ± 0.34[b]	5.94e-04	0.008
SOD, U/ml	7.69 ± 1.06[a]	6.18 ± 1.85[a]	6.67 ± 0.64[a]	6.49 ± 0.56[a]	0.016	0.105
GSH-Px	180.64 ± 6.10[a]	170.98 ± 16.66[a]	179.53 ± 11.83[a]	177.26 ± 7.24[a]	0.298	0.655
GSH, μmol/ml	0.41 ± 0.02[a]	0.41 ± 0.06[a]	0.42 ± 0.03[a]	0.44 ± 0.06[a]	0.440	0.655
IL-1β, ng/l	123.34 ± 22.56[a]	113.28 ± 17.38[a]	103.06 ± 24.14[a]	94.89 ± 29.95[a]	0.103	0.444
IL-2, ng/l	97.96 ± 29.26[a]	95.65 ± 24.03[a]	112.28 ± 27.94[a]	103.91 ± 29.01[a]	0.489	0.655
IL-4, pg/ml	114.97 ± 21.57[a]	108.48 ± 19.06[a]	99.80 ± 20.84[a]	103.08 ± 24.14[a]	0.504	0.655
IL-10, ng/l	134.34 ± 33.92[a]	162.89 ± 41.53[a]	158.07 ± 24.91[a]	151.80 ± 35.08[a]	0.316	0.655
IgA, μg/ml	18.78 ± 3.73a	18.59 ± 5.32[a]	19.27 ± 2.71[a]	18.03 ± 4.00[a]	0.870	0.870
IgM, μg/ml	9.50 ± 1.78[a]	9.13 ± 2.43[a]	9.01 ± 2.66[a]	8.70 ± 2.14[a]	0.867	0.870
IFN-γ, ng/l	40.51 ± 11.14[a]	42.54 ± 6.44[a]	34.44 ± 4.37[a]	40.76 ± 13.34[a]	0.379	0.655
TNF-α, ng/l	616.15 ± 166.83[a]	575.93 ± 113.29[a]	632.77 ± 147.08[a]	536.71 ± 161.35[a]	0.561	0.663

CTRL – conventional-protein control diet, LPD – low-protein diet, LPDL – low-protein diet supplemented with rumen-protected lysine, LPDM – low-protein diet supplemented with rumen-protected methionine, CAT – catalase, SOD – superoxide dismutase, GSH-Px – glutathione peroxidase, GSH – reduced glutathione, IL – interleukin, IgA – immunoglobulin A, IgM – immunoglobulin M, IFN-γ – interferon gamma, TNF-α – tumour necrosis factor alpha, FDR – false discovery rate. Values are presented as mean ± standard deviation (SD). The *P*-values were obtained using Kruskal-Wallis tests, and the q-values are Benjamini-Hochberg false discovery rate (FDR)-adjusted values. Different superscript letters within a row indicate significant post-hoc differences among dietary treatments at $q < 0.05$; identical letters indicate no significant difference.

Figure 1. Experimental housing of growing male Hu sheep during the feeding trial.

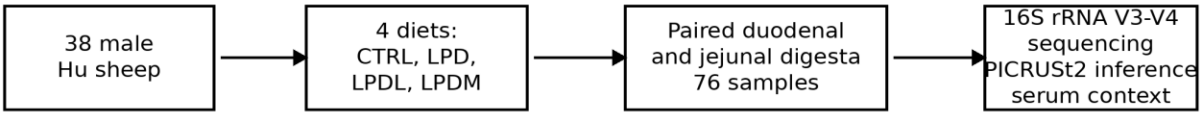

Figure 2. Experimental design and analytical workflow for the paired duodenal and jejunal digesta microbiome study. Thirty-eight growing male Hu sheep were assigned to four dietary treatments. Each animal provided one duodenal and one jejunal digesta sample, yielding 76 microbiome samples arranged as 38 paired duodenal–jejunal sample sets. Samples underwent 16S rRNA V3–V4 sequencing and PICRUSt2 functional inference, while serum variables were evaluated as supportive host-response context.

CTRL – conventional-protein control diet, LPD – low-protein diet, LPDL – low-protein diet supplemented with rumen-protected lysine, LPDM – low-protein diet supplemented with rumen-protected methionine, rRNA – ribosomal RNA, PICRUSt2 – Phylogenetic Investigation of Communities by Reconstruction of Unobserved States 2

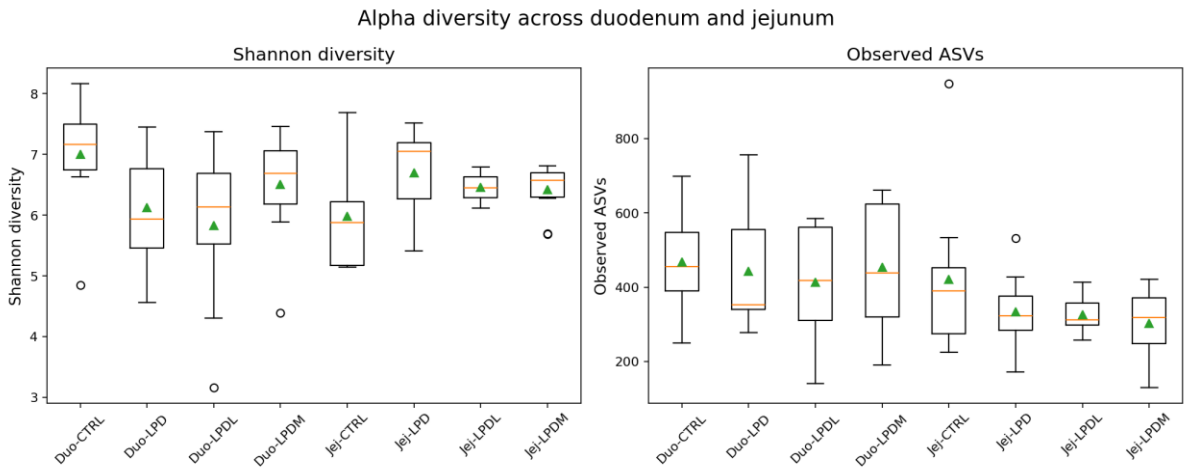

Figure 3. Alpha-diversity patterns in duodenal and jejunal digesta samples across dietary treatments. Boxplots show the Shannon diversity index and the number of observed amplicon sequence variants (ASVs) for each intestinal segment and dietary treatment. Horizontal lines within boxes indicate medians, green triangles indicate means, boxes represent interquartile ranges, whiskers indicate data ranges excluding outliers, and circles represent outliers.

CTRL – conventional-protein control diet, LPD – low-protein diet, LPDL – low-protein diet supplemented with rumen-protected lysine, LPDM – low-protein diet supplemented with rumen-protected methionine, Duo – duodenum, Jej – jejunum, ASVs – amplicon sequence variants

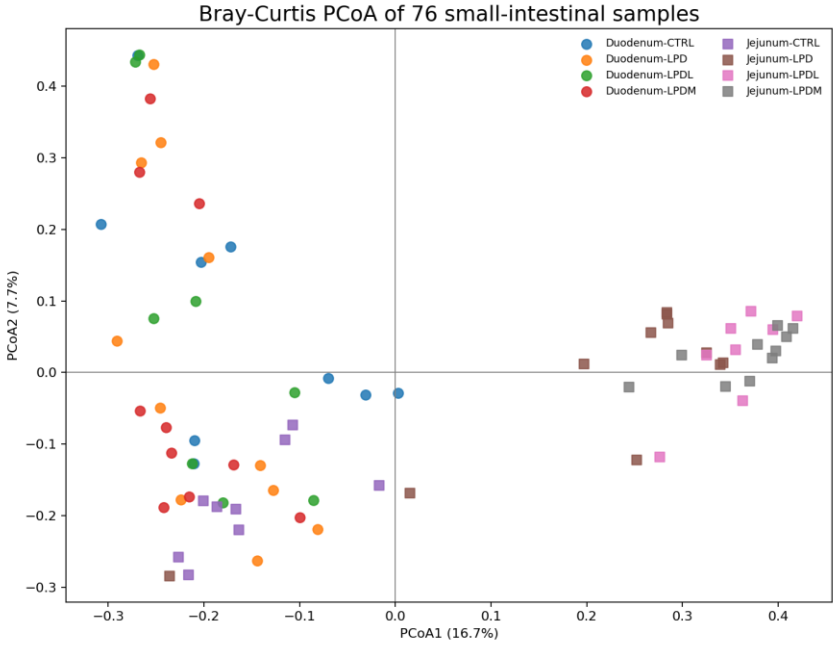

Figure 4. Principal coordinate analysis of microbial community structure in paired duodenal and jejunal digesta samples. Principal coordinate analysis (PCoA) based on Bray-Curtis dissimilarity shows the distribution of 76 microbiome samples according to intestinal segment and dietary treatment. PCoA1 and PCoA2 explained 16.7% and 7.7% of the total variation, respectively. Circles represent duodenal samples, squares represent jejunal samples, and colours distinguish the four dietary treatments.

CTRL – conventional-protein control diet, LPD – low-protein diet, LPDL – low-protein diet supplemented with rumen-protected lysine, LPDM – low-protein diet supplemented with rumen-protected methionine, PCoA – principal coordinate analysis

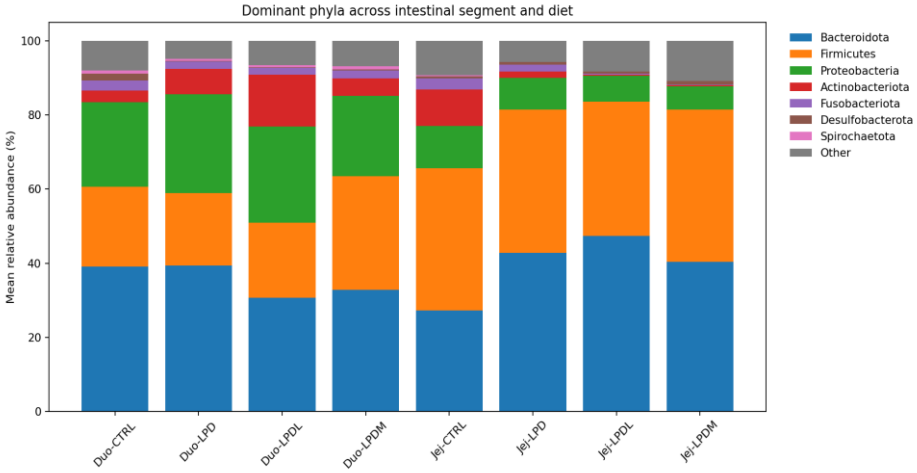

Figure 5. Relative abundance of dominant bacterial phyla in duodenal and jejunal digesta samples across dietary treatments. The stacked bar chart shows the mean relative abundance (%) of dominant bacterial phyla in duodenal and jejunal samples from the four dietary groups.

CTRL – conventional-protein control diet, LPD – low-protein diet, LPDL – low-protein diet supplemented with rumen-protected lysine, LPDM – low-protein diet supplemented with rumen-protected methionine, Duo – duodenum, Jej – jejunum

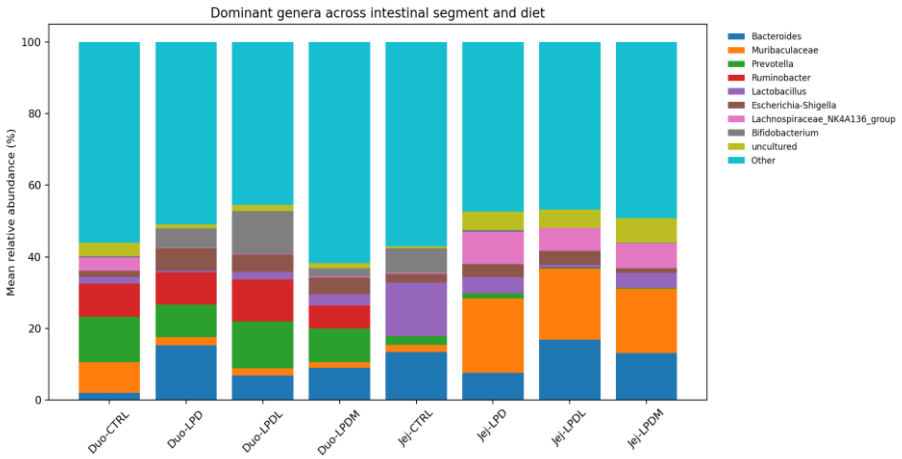

Figure 6. Relative abundance of dominant bacterial genera in duodenal and jejunal digesta samples across dietary treatments. The stacked bar chart shows the mean relative abundance (%) of the dominant bacterial genera in duodenal and jejunal samples from the four dietary groups.

CTRL – conventional-protein control diet, LPD – low-protein diet, LPDL – low-protein diet supplemented with rumen-protected lysine, LPDM – low-protein diet supplemented with rumen-protected methionine, Duo – duodenum, Jej – jejunum

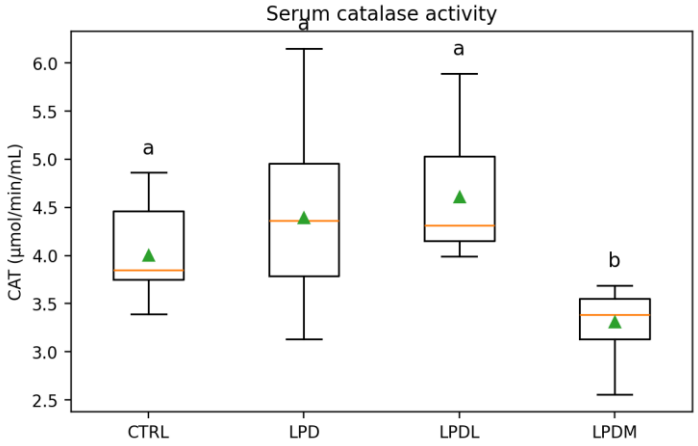

Figure 7. Serum catalase activity in growing Hu sheep across dietary treatments. Boxplots show serum CAT activity in the four dietary groups. Different lowercase letters indicate significant post-hoc differences after Benjamini–Hochberg false discovery rate adjustment at $q < 0.05$; groups sharing the same letter did not differ significantly. Statistical results are presented in Table 6.

CTRL – conventional-protein control diet, LPD – low-protein diet, LPDL – low-protein diet supplemented with rumen-protected lysine, LPDM – low-protein diet supplemented with rumen-protected methionine, CAT – catalase, FDR – false discovery rate

Supplementary material

Supplementary Table S1 provides detailed information on serum assay kits, including manufacturer, catalogue number, assay principle, detection wavelength where applicable, and intra-/inter-assay coefficients of variation.

Supplementary Table S2 presents growth performance and feed efficiency parameters of the 38 sequenced animals.

Supplementary Table S3 summarizes nutrient digestibility coefficients across dietary treatments.

Supplementary Table S4 includes rumen fermentation characteristics and volatile fatty acid profiles.

Supplementary Table S5 presents dominant phyla across duodenal and jejunal samples by dietary treatment.

Supplementary Figure S1 presents rarefaction curves for duodenal and jejunal digesta samples, including observed ASVs and Shannon diversity metrics.

Supplementary Table S1. Biochemical, antioxidant, and immune-related assays used for serum parameter determination

Indicator	Kit / assay	Manufacturer	Detection range / method
Glucose	ADS-W-TDX002, GOPOD oxidase microplate method	Jiangsu Addison Biotechnology Co., Ltd.	520 nm
CAT	ADS-W-KY002-48, microplate method	Jiangsu Addison Biotechnology Co., Ltd.	510 nm
SOD	ADS-W-KY011-48, WST-8 microplate method	Jiangsu Addison Biotechnology Co., Ltd.	450 nm
GSH-Px	ADS-W-G003-48, microplate method	Jiangsu Addison Biotechnology Co., Ltd.	412 nm
GSH	ADS-W-G001-48, DTNB microplate method	Jiangsu Addison Biotechnology Co., Ltd.	412 nm
IgA	Sheep IgA ELISA	Jiangsu Meimian Industrial Co., Ltd.	0.8–24 μg/ml
IgM	Sheep IgM ELISA	Jiangsu Meimian Industrial Co., Ltd.	0.2–18 μg/ml
IL-1β	Sheep IL-1β ELISA	Jiangsu Meimian Industrial Co., Ltd.	3–120 ng/l
IL-2	Sheep IL-2 ELISA	Jiangsu Meimian Industrial Co., Ltd.	3–150 ng/l
IL-4	Sheep IL-4 ELISA	Jiangsu Meimian Industrial Co., Ltd.	5–125 pg/ml
IL-10	Sheep IL-10 ELISA	Jiangsu Meimian Industrial Co., Ltd.	7–200 ng/l
TNF-α	Sheep TNF-α ELISA	Jiangsu Meimian Industrial Co., Ltd.	25–800 ng/l
IFN-γ	Sheep IFN-γ ELISA	Jiangsu Meimian Industrial Co., Ltd.	2–50 ng/l

CAT – catalase, SOD – superoxide dismutase, GSH-Px – glutathione peroxidase, GSH – reduced glutathione, IgA – immunoglobulin A, IgM – immunoglobulin M, IL-1β – interleukin-1 beta, IL-2 – interleukin-2, IL-4 – interleukin-4; IL-10 – interleukin-10, TNF-α – tumour necrosis factor alpha, IFN-γ – interferon gamma, ELISA – enzyme-linked immunosorbent assay, GOPOD – glucose oxidase–peroxidase, WST-8 – water-soluble tetrazolium salt-8; DTNB – 5,5'-dithiobis(2-nitrobenzoic acid). For biochemical and antioxidant assays, the values in the final column indicate

detection wavelengths; for enzyme-linked immunosorbent assay (ELISA) kits, they indicate detection ranges. All assays were performed according to the manufacturers' instructions. The reported intra-assay and inter-assay coefficients of variation were <10% and <15%, respectively.

Supplementary Table S2. Growth performance, feed intake, and feed conversion of the 38 sequenced sheep

Variable	CTRL	LPD	LPDL	LPDM	*P*-value
Initial body weight, kg	23.84 ± 1.82	23.87 ± 2.02	24.62 ± 1.77	24.27 ± 2.19	0.801
Final body weight, kg	36.91 ± 3.53	35.55 ± 3.45	38.44 ± 3.09	36.48 ± 3.22	0.423
Average daily gain, g/day	277.90 ± 53.08	248.45 ± 47.29	293.88 ± 35.76	259.89 ± 31.60	0.108
Dry matter intake, kg/day	1.512 ± 0.194	1.444 ± 0.153	1.588 ± 0.185	1.496 ± 0.188	0.499
Feed conversion ratio	5.49 ± 0.36	5.93 ± 0.75	5.41 ± 0.29	5.77 ± 0.39	0.103

CTRL, conventional-protein control diet; LPD, low-protein diet; LPDL, low-protein diet supplemented with rumen-protected lysine; LPDM – low-protein diet supplemented with rumen-protected methionine, SD – standard deviation. Values are presented as mean ± SD. Group sizes were CTRL, n = 9; LPD, n = 11; LPDL, n = 8; and LPDM, n = 10. The *P*-values were obtained using Kruskal-Wallis tests. None of the growth-performance or feed-efficiency variables differed significantly among dietary treatments ($P > 0.05$). These data were included as supportive nutritional context rather than primary study endpoints.

Supplementary Table S3. Apparent nutrient digestibility of the 38 sequenced sheep across dietary treatments

Variable	CTRL	LPD	LPDL	LPDM	*P*-value
Dry matter digestibility, %	22.34 ± 9.94	34.84 ± 6.27	29.38 ± 19.64	51.11 ± 5.10	<0.001
Organic matter digestibility, %	48.50 ± 8.20	62.32 ± 5.85	55.17 ± 17.84	75.54 ± 4.46	<0.001
Crude protein digestibility, %	69.83 ± 4.06	71.95 ± 4.16	67.29 ± 13.55	81.98 ± 3.41	<0.001
Neutral detergent fibre digestibility, %	25.48 ± 11.82	42.54 ± 9.09	33.09 ± 26.93	63.38 ± 6.87	<0.001
Acid detergent fibre digestibility, %	31.24 ± 9.53	42.90 ± 7.88	32.09 ± 26.83	62.59 ± 6.15	<0.001
Starch digestibility, %	97.15 ± 2.90	98.40 ± 0.79	98.60 ± 0.55	98.53 ± 0.88	0.246
Ether extract digestibility, %	81.04 ± 6.56	83.06 ± 5.39	76.78 ± 11.64	90.05 ± 3.40	0.005

CTRL – conventional-protein control diet, LPD – low-protein diet, LPDL – low-protein diet supplemented with rumen-protected lysine, LPDM – low-protein diet supplemented with rumen-protected methionine, SD – standard deviation. Values are presented as mean ± SD. Group sizes were CTRL, n = 9; LPD, n = 11; LPDL, n = 8; and LPDM, n = 10. The *P*-values were obtained using Kruskal-Wallis tests. A *P*-value <0.05 was considered statistically significant. Apparent digestibility differed significantly among dietary treatments for dry matter, organic matter, crude protein, neutral detergent fibre, acid detergent fibre, and ether extract, whereas starch digestibility did not differ significantly. These data were included as supportive nutritional context rather than primary study endpoints.

Supplementary Table S4. Rumen fermentation characteristics of the 38 sequenced sheep across dietary treatments

Variable	CTRL	LPD	LPDL	LPDM	*P*-value

Rumen pH	5.97 ± 0.28	5.95 ± 0.38	6.27 ± 0.40	5.96 ± 0.27	0.252
Total VFA, mM	45.15 ± 11.23	47.69 ± 12.91	39.63 ± 8.47	43.32 ± 13.00	0.360
Acetate, mM	19.10 ± 3.98	18.64 ± 4.66	16.29 ± 2.59	18.02 ± 5.68	0.557
Propionate, mM	14.87 ± 4.29	18.37 ± 4.74	14.90 ± 6.14	15.90 ± 6.32	0.226
Butyrate, mM	9.10 ± 3.91	8.81 ± 3.91	6.86 ± 2.83	7.62 ± 2.86	0.539
Acetate: propionate ratio	1.33 ± 0.28	1.03 ± 0.17	1.19 ± 0.32	1.20 ± 0.31	0.123

CTRL – conventional-protein control diet, LPD – low-protein diet, LPDL – low-protein diet supplemented with rumen-protected lysine, LPDM – low-protein diet supplemented with rumen-protected methionine, VFA – volatile fatty acids, SD – standard deviation. Values are presented as mean ± SD. Group sizes were CTRL, n = 9; LPD, n = 11; LPDL, n = 8; and LPDM, n = 10. The *P*-values were obtained using Kruskal-Wallis tests. No rumen fermentation variable differed significantly among dietary treatments ($P > 0.05$). These measurements were included as supportive nutritional context rather than primary study endpoints.

Supplementary Table S5. Relative abundance of dominant bacterial phyla in duodenal and jejunal digesta samples across dietary treatments

Phylum	Overall mean, %	Duodenum (CTRL; LPD; LPDL; LPDM)	Jejunum (CTRL; LPD; LPDL; LPDM)	Segment *P* / q
Bacteroidota	37.60	CTRL: 38.99 ± 4.44; LPD: 39.29 ± 5.32; LPDL: 30.68 ± 18.31; LPDM: 32.77 ± 8.63	CTRL: 27.23 ± 11.99; LPD: 42.86 ± 16.51; LPDL: 47.59 ± 7.32; LPDM: 40.43 ± 10.46	0.204 / 0.448
Firmicutes	30.90	CTRL: 21.70 ± 10.41; LPD: 19.68 ± 7.70; LPDL: 20.15 ± 7.64; LPDM: 30.64 ± 11.15	CTRL: 38.41 ± 20.87; LPD: 38.58 ± 15.22; LPDL: 36.07 ± 11.57; LPDM: 41.06 ± 11.49	1.39e-07 / 2.57e-06
Proteobacteria	16.33	CTRL: 22.83 ± 15.06; LPD: 26.62 ± 12.51; LPDL: 26.02 ± 11.91; LPDM: 21.74 ± 7.47	CTRL: 11.51 ± 7.19; LPD: 8.57 ± 11.78; LPDL: 7.04 ± 7.83; LPDM: 6.27 ± 2.56	9.44e-08 / 2.57e-06
Other	6.27	CTRL: 6.00 ± 4.49; LPD: 3.61 ± 2.71; LPDL: 5.52 ± 6.22; LPDM: 5.66 ± 4.04	CTRL: 8.05 ± 3.13; LPD: 4.36 ± 2.06; LPDL: 7.60 ± 4.54; LPDM: 10.05 ± 8.07	0.036 / 0.132
Actinobacteriota	4.97	CTRL: 3.11 ± 3.42; LPD: 6.87 ± 7.34; LPDL: 14.12 ± 21.55; LPDM: 4.78 ± 4.56	CTRL: 9.84 ± 8.09; LPD: 1.68 ± 2.57; LPDL: 0.32 ± 0.21; LPDM: 0.36 ± 0.33	0.036 / 0.132
Fusobacteriota	1.74	CTRL: 2.79 ± 3.53; LPD: 1.98 ± 3.60; LPDL: 1.78 ± 3.48; LPDM: 2.04 ± 1.97	CTRL: 2.98 ± 3.64; LPD: 1.89 ± 4.01; LPDL: 0.22 ± 0.18; LPDM: 0.17 ± 0.12	0.016 / 0.075
Desulfobacterota	0.65	CTRL: 1.82 ± 3.04; LPD: 0.11 ± 0.06;	CTRL: 0.60 ± 1.04; LPD: 0.73 ± 0.69;	0.004 / 0.019

Spirochaetota	0.39	LPDL: 0.15 ± 0.09; LPDM: 0.34 ± 0.35 CTRL: 0.79 ± 0.73; LPD: 0.60 ± 0.61; LPDL: 0.62 ± 0.75; LPDM: 0.80 ± 0.82	LPDL: 0.56 ± 0.27; LPDM: 0.90 ± 0.77 CTRL: 0.27 ± 0.45; LPD: 0.01 ± 0.02; LPDL: 0.03 ± 0.07; LPDM: 0.01 ± 0.01	4.05e-06 / 3.75e-05

CTRL – conventional-protein control diet, LPD – low-protein diet, LPDL – low-protein diet supplemented with rumen-protected lysine, LPDM – low-protein diet supplemented with rumen-protected methionine, FDR – false discovery rate, SD – standard deviation. Values are presented as mean relative abundance (%) ± SD. The overall mean represents the average relative abundance across all 76 samples. Segment *P*-values were obtained from paired duodenum-jejunum comparisons, and segment q-values are Benjamini-Hochberg false discovery rate (FDR)-adjusted values. Statistical significance was defined as $q < 0.05$.

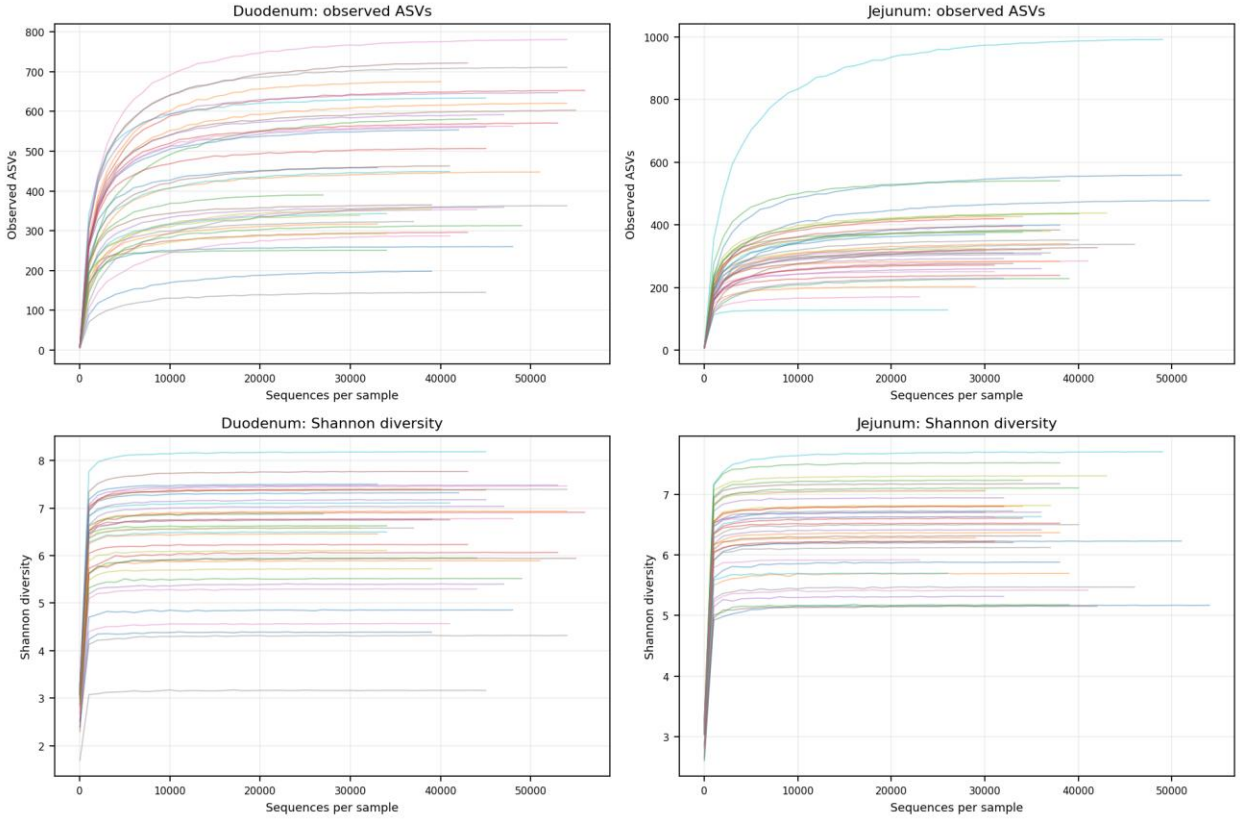

Supplementary Figure S1. Rarefaction curves for paired duodenal and jejunal digesta samples. Curves show the relationship between sequencing depth and observed amplicon sequence variants (ASVs) and Shannon diversity in duodenal and jejunal samples. The approach of the curves toward plateaus indicates adequate sequencing depth for downstream microbial diversity analyses. ASVs, amplicon sequence variants.